J Biol Inorg Chem (2008) 13:813–824
DOI 10.1007/s00775-008-0368-5

ORIGINAL PAPER

The effect of mutation of F87 on the properties of CYP102A1-CYP4C7 chimeras: altered regiospecificity and substrate selectivity

Chiung-Kuang J. Chen · Tatiana Kh. Shokhireva · Robert E. Berry · Hongjun Zhang · F. Ann Walker

Received: 24 November 2007 / Accepted: 20 March 2008 / Published online: 8 April 2008

Abstract CYP102A1 is a highly active water-soluble bacterial monooxygenase that contains both substrate-binding heme and diflavin reductase subunits, all in a single polypeptide that has been called a "self-sufficient enzyme." Several years ago we developed a procedure called "scanning chimeragenesis," where we focused on residues 73–82 of CYP102A1, which contact approximately 40% of the substrates palmitoleic acid and *N*-palmitoylglycine [Murataliev et al. (2004) Biochemistry 43:1771–1780]. These residues were replaced with the homologous residues of CYP4C7. In the current work, that study has been expanded to include residue 87. Phenylalanine 87 of wild-type CYP102A1 was replaced with the homologous residue of CYP4C7, leucine, as well as with alanine. The full-sized chimeric proteins C(73–78, F87L), C(73–78, F87A), C(75–80, F87L), C(75–80, F87A), C(78–82, F87L) and C(78–82, F87A) have been purified and characterized. Wild-type CYP102A1 is most active toward fatty acids (both lauric and palmitic acids produce ω-1, ω-2, and ω-3 hydroxylated fatty acids), but it also catalyzes the oxidation of farnesol to three products (2, 3- and 10,11-epoxyfarnesols and 9-hydroxyfarnesol). All of the F87-mutant chimeric proteins show dramatic decreases in activities with the natural CYP102A1 substrates. In contrast, C(78–82, F87A) and C(78–82, F87L) have markedly increased activities with farnesol, with the latter showing a 5.7-fold increase in catalytic activity as compared to wild-type CYP102A1. C(78–82, F87L) produces 10,11-epoxyfarnesol as the single primary metabolite. The results show that chimeragenesis involving only the second half of SRS-1 plus F87 is sufficient to change the substrate selectivity of CYP102A1 from fatty acids to farnesol and to produce a single primary product.

Keywords Cytochrome · Heme · Site-directed mutagenesis

Abbreviations

CYP102A1	Cytochrome P450 from *Bacillus megaterium*, also called P450-BM3
CYP4C7	A membrane-bound cytochrome P450 from the cockroach, *Diploptera punctata*

Introduction

CYP102A1 (also called P450 BM3) is a "self-sufficient" monooxygenase from *Bacillus megaterium* [1–7] that is a bacterial class II [7] cytochrome P450 enzyme. It contains a heme domain fused to a FAD/FMN diflavin reductase [8] domain in a single 119-kDa polypeptide [1, 4]. In the presence of NADPH and O_2, this soluble enzyme can catalyze the hydroxylation of medium- and long-chain fatty acids such as lauric, myristic, palmitic, and stearic acids (Scheme 1) at the ω-1, ω-2, and ω-3 carbons [1, 2] and epoxidize double bonds stereospecifically [9]. Its fusion of the heme and reductase domains affords monooxygenation of saturated or unsaturated fatty acids with the highest catalytic activities among any of the P450

Electronic supplementary material The online version of this article (doi:10.1007/s00775-008-0368-5) contains supplementary material, which is available to authorized users.

C.-K. J. Chen · T. Kh. Shokhireva · R. E. Berry · H. Zhang · F. A. Walker (✉)
Department of Chemistry,
University of Arizona,
Tucson, AZ 85721-0041, USA
e-mail: awalker@u.arizona.edu

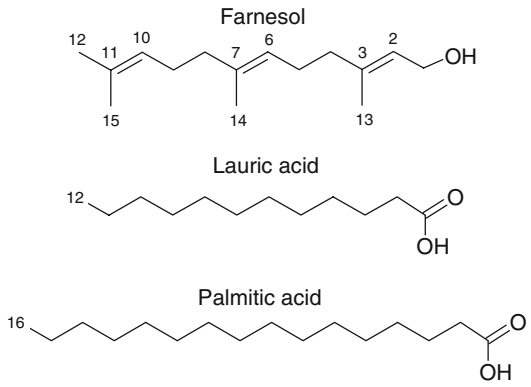

Scheme 1 Structural formulae of farnesol, lauric acid and palmitic acid

monooxygenases [3, 10]. CYP102A1 has attracted researchers' attention as a template for engineering new enzymes that have modified regio- and stereospecificities and/or substrate selectivities for biotechnological and biomedical uses [9–17].

Several structures of the heme domain of CYP102A1 have been reported [18–23], two of which have substrate—either palmitoleic acid or *N*-palmitolyl glycine bound to the ferriheme state of the enzyme [19, 21]. A puzzling feature of these structures is the fact that the closest approach of substrate to the heme iron is 7.75 Å [19, 21]. In agreement with this large distance, NMR paramagnetic relaxation studies of the substrate-bound form of the ferriheme domain of CYP102A1 [24] have shown that in the ferric form the substrate is much too far from the heme iron for the hydroxylation reaction to occur. However, upon one-electron reduction the substrate moves about 6 Å closer to the ferrous iron center [25], indicating a change in the structure of the substrate binding channel upon reduction of heme iron. The complete 3-D structure of the substrate-bound ferrous form of the heme domain of CYP102A1 is not known.

Site-directed mutagenesis and directed evolution have been used [10, 14, 26–45] to produce modified P450 enzymes with altered catalytic activities and regio- and stereospecificities. In our laboratory, "scanning chimeragenesis" was developed to introduce peptide sequences from a P450 enzyme for which no crystal structure is available into homologous regions of CYP102A1 as a way of changing substrate selectivity and regiospecificity [46]. The insect cytochrome P450 enzyme CYP4C7, isolated from *Diploptera punctata* (the cockroach) [47], was selected for peptide sequence replacement because one of its substrates, farnesol (shown in Scheme 1), is also a substrate of CYP102A1, but the two enzymes produce different products [46, 47]. Farnesol is known as a precursor of methyl 9,10-epoxyfarnesoate, also known as juvenile hormone III (JH III), which exists in cockroaches and mosquitoes [47–53]. The primary function of JH III is the control of insect development, metamorphosis and reproduction [47, 49, 53]. CYP4C7 reacts with farnesol to produce 12-hydroxyfarnesol as the primary metabolite [47], while CYP102A1 catalyzes the oxidation of farnesol to a mixture of 2,3- and 10,11-epoxyfarnesol as well as 9-hydroxyfarnesol [46, 54]. The goal of this project is to produce an active enzyme, using the CYP102A1 scaffold, which catalyzes the oxidation of farnesol to 12-hydroxyfarnesol.

The "scanning chimeragenesis" experimental approach began with the identification of individual structural elements of CYP102A1 that participate in substrate recognition and binding to the typical substrates of that enzyme, and their replacement with the homologous peptides of CYP4C7 [46]. In order to identify the sites, the sequence of CYP102A1, for which two X-ray structures of the heme domain with bound substrate are known [19, 21], was aligned with that of CYP4C7, for which no structure is available, using the GAP program of the GCG package (http://www.accelrys.com/products/gcg/) and FASTA3 [55]. This alignment was used with the crystal structures [19, 21] to identify substrate-interacting residues of CYP4C7 to be considered for replacement in CYP102A1. Originally those within 7 Å of the substrate were used [46], but in this study we have focused on those within 5 Å of the substrates. Many of the residues within that distance were found to be within the substrate recognition sites (SRS) of CYP102A1, and the highest concentration was within SRS-1 and several residues that follow it.

Residues inferred as being a part of the SRS have been identified by X-ray crystallography of substrate-bound forms of cytochromes P450, initially of the CYP2 family [56], but now all CYP enzymes, including CYP102A1 [14]. SRS-1–6 are located along the primary sequence of the CYP enzymes, and constitute about 16% of the total residues [56]. They occur in structurally homologous regions of the amino acid sequence, although there is little or no conservation of amino acid *identity* from one P450 to another.

A study of a series of B′-helix chimeric proteins using portions of residues 73–82 has been published [46]. It shows that the chimeras C(73–78), C(75–80) and C(78–82) change the regioselectivity of the enzyme to produce new metabolites that were identified as 10-hydroxypalmitic acid and 5-hydroxyfarnesol. Neither of these metabolites are produced by wild-type CYP102A1. One, C(75–80), even had 5-hydroxyfarnesol as the primary product, with only trace amounts of the 9-hydroxy derivative [46]. For the longest chimera, C(73–84), farnesol and palmitate oxidation were inhibited by one and four orders of magnitude,

respectively [46]. In that work, "scanning" chimeragenesis was stopped at residue 82 because the residues identified as SRS-1 and the B′-helix ended with G83. This residue is common to both CYP102A1 and CYP4C7, although two additional residues in the loop that follows, F87 and T88, were shown to be within 5 Å of the substrate *N*-palmitoylglycine [20], while only F87 was within 5 Å of palmitoleic acid [18]. T88 is common to both CYP102A1 and CYP4C7, but F87 is unique to CYP102A1. The corresponding residue is a leucine in CYP4C7.

F87 has long been of interest to researchers who have studied CYP102A1 because of its proximity to the heme iron and the orientation of its phenyl ring. In the substrate-free structure, the F87 phenyl ring is nearly perpendicular to the heme plane [18], but it is within 45° of the heme plane in the substrate-bound structures, and seems to block access of the substrate to the heme active site [19, 21]. Three point mutants have previously been reported, F87V, Y [17, 26] and A [28], and the A mutant in particular has been discussed in view of the structure of the heme domain bound to palmitoleic acid [10, 17, 57]. It was found that while wild-type CYP102A1 produced the 18(*R*) hydroxy and 14(*S*),15(*R*)-epoxy metabolites of arachidonic acid [9], CYP102A1-F87Y produced an inactive protein [26] and CYP102A1-F87V produced a highly regio- and stereoselective arachidonic acid epoxygenase by producing 99% (14*S*,15*R*)-epoxyeicosatrienoic acid [26]. CYP102A1-F87A was found to be an ω-hydroxylase of shorter chain fatty acids, and was reported to produce >90% 12-hydroxylauric acid and 14-hydroxymyristic acid [28], but there has been no report of its activity with palmitic acid or with farnesol.

In this work we have extended the previous study [46] to produce seven new functional point mutant proteins, CYP102A1-F87L, C(73–78, F87L), C(73–78, F87A), C(75–80, F87L), C(75–80, F87A), C(78–82, F87L) and C(78–82, F87A), where the numbers indicate the residues of CYP102A1 that have been replaced with the homologous residues of CYP4C7 [46], with sequences shown in Table 1. In addition, we again prepared the previously reported CYP102A1-F87A mutant [28] for comparison, and found somewhat different results. Based on the activity results for the newly prepared proteins with the substrates lauric and palmitic acid and farnesol, a catalytically more active (toward farnesol) chimeric protein than wild-type CYP102A1 has been produced, with new regiospecificity and altered substrate selectivity.

Table 1 Amino acid sequences of CYP4C7, CYP102A1 and the amino acid replacements in the mutant proteins of this study (shown underlined)

Protein	Sequence
CYP4C7 (96–113)	SYEYSFLFPWLGTGLLTS
CYP102A1 (72–89)	SQALKFVRDFAGDGLFTS
F87A[a]	SQALKFVRDFAGDGLATS
F87L[a]	SQALKFVRDFAGDGLLTS
C(73–78)[b]	SYEYSFLRDFAGDGLFTS
C(73–78, F87A)[a]	SYEYSFLRDFAGDGLATS
C(73–78, F87L)[a]	SYEYSFLRDFAGDGLLTS
C(75–80)[b]	SQAYSFLFPFAGDGLFTS
C(75–80, F87A)[a]	SQAYSFLFPFAGDGLATS
C(75–80, F87L)[a]	SQAYSFLFPFAGDGLLTS
C(78–82)[b]	SQALKFLFPWLGDGLFTS
C(78–82, F87A)[a]	SQALKFLFPWLGDGLATS
C(78–82, F87L)[a]	SQALKFLFPWLGDGLLTS

[a] Prepared in this work

[b] Prepared in [46] and again in this work

Materials and methods

All primers were obtained from Operon (Huntsville, AL, USA). The polymerase and restriction enzymes were ordered from Bio-Labs (Ipswich, MA, USA). PCR reactions were incubated in a programmable thermal controller, the PTC-100 from MJ Research (Ramsey, MN, USA). All samples containing product mixtures for identification were injected into a Hewlett–Packard 5890 Series II gas chromatograph with a flame ionization detector and a a 30-m DB-1 capillary column (J&W, Agilent, Santa Clara, CA, USA). GC–MS samples were investigated by electron impact using a Varian Saturn 2000 (Walnut Creek, CA, USA) gas chromatograph–mass spectrometry system. The gas chromatography column was a Hewlett–Packard (Palo Alto, CA, USA) HP-5 ms with a length of 30 m, an internal diameter of 0.25 mm, and a film thickness of 0.33 μm. The mass spectra were collected using electron ionization at 70 eV. MALDI-TOF spectra were obtained on a Bruker (Billerica, MA, USA) Reflex-III MALDI/TOF spectrometer. Absorption spectra were recorded on a Perkin–Elmer (Wellesley, MA, USA) Lamda 19 UV/vis spectrophotometer. Inductively coupled plasma (ICP) atomic emission spectrometry measurements of the iron and sulfur contents of the proteins were made on a Thermo Jarrell Ash Corp. (Franklin, MA, USA) IRIS Advantage ICP 2000. The solvents used for all experiments were HPLC or higher grade. NMR spectra, both 1-D and COSY spectra, were obtained on a Bruker DRX-600 spectrometer operating at 600.03 MHz for the proton Larmor frequency. Spectra were collected at 25 °C with the proton chemical shifts referenced to residual solvent (CD_3OD) CD_2H. Two-dimensional NMR spectra were collected with 2,048 data points in t_2 and with 256–512 blocks in t_1 with 32–64 scans/block.

Mutant gene preparation, protein expression and purification

The amino acid sequences of CYP102A1 and CYP4C7 for the region encompassing SRS-1 and the loop that follows, together with the amino acid replacements for the mutant proteins, are shown in Table 1. The mutant protein expression and purification followed the protocols published previously [58], and are described in detail in the "Electronic supplementary material," along with Fig. S1 and Table S1. Although these could be considered point mutations, the preparation of the mutant genes was not accomplished in this way. Rather, as shown in the "Electronic supplementary material," all of the codons for the original chimera, including the codons for amino acid 87, were replaced in each case using standard genetic engineering methods [46, 58, 59]. The proteins were expressed in *Escherichia coli* as described previously [46]. The mutations were confirmed by DNA sequencing and the expressed proteins were judged to be homogeneous by SDS-PAGE (Bio-Rad, Hercules, CA, USA). These proteins were preliminarily characterized by ICP atomic emission, UV/visible and mass spectrometry (MALDI–TOF). In addition, all proteins were expressed, purified and characterized in two separate batches in order to confirm the reproducibility of the protein preparation. The final purified proteins were extensively dialyzed against 50 mM potassium phosphate buffer (pH 7.6), concentrated, and then stored at −20 °C in 50% glycerol.

ICP atomic emission spectrometry

The iron and sulfur content of CYP102A1 and its mutants were measured by ICP atomic emission spectrometry [60]. All solutions were prepared in DDI water at 25 °C, and standardized solutions of 0.1–10 ppm iron and 0.1–20 ppm sulfur were prepared to generate calibration curves. Dilution and background errors were estimated and found to be much smaller than the scatter in the experimental data. All S and Fe concentration measurements in each protein sample were repeated 12 times for accuracy and consistency. The results are presented in the "Electronic supplementary material," Table S2.

UV/visible spectroscopy

The resting state spectra were recorded as reported previously [3, 5, 46] and are shown in the "Electronic supplementary material," Fig. S2. The CO-bound difference spectra of the dithionite-reduced proteins were measured, as reported previously [3, 5, 7], and are comparable to those of other cytochromes P450 [61, 62] (which lack the diflavin reductase domain). Using argon purged buffers (200 mM Tris–HCl buffer at pH 7.7) a solution of each protein (1 μM in 3 mL) was reduced with 20 μL of a saturated solution of sodium dithionite (freshly prepared in the same buffer) and the spectrum was recorded. Then 20 μL aliquots of a saturated solution of CO in the same buffer (calculated from its solubility at ∼800 μM) were added to the solution (at 25 °C) with mixing. The spectrum was recorded again following each addition until there was no further change in the spectrum (results presented in the "Electronic supplementary material," Fig. S3) [3, 5, 7, 61, 62].

Enzyme activity assays for cytochrome *c* reduction and NADPH oxidation

To measure the reductase activity, the absorbance at 550 nm ($\varepsilon_{ox} = 8.9\ mM^{-1}\ cm^{-1}$, $\varepsilon_{red} = 29.9\ mM^{-1}\ cm^{-1}$ [5]) was followed for 1-mL samples containing 2 nM enzyme and 50 μM oxidized cytochrome *c* containing the NADPH-regenerating system (1.0 mM glucose-6-phosphate, 3.0 U mL^{-1} glucose-6-phosphate dehydrogenase, and 50 μM NADPH). This was repeated for a solution containing no enzyme, and the difference in rate was reported [5, 6, 58]. NADPH oxidation was measured in the presence of 10 nM enzyme, 100 μM nucleotide, 50 μM oxidized cytochrome *c* and 200 μM laurate by following the decrease in absorbance at 340 nm and using an extinction coefficient of 6.22 $mM^{-1}\ cm^{-1}$ [58]. The enzyme activities with cytochrome *c*, NADPH, lauric and palmitic acid and farnesol are shown in Table 2.

Enzyme activity assays for farnesol, lauric and palmitic acid

All enzyme incubations and activity assays were carried out at 25 °C in 3-mL volumes (containing 100 mM Tris–HCl pH 7.6 buffer and the NADPH-regenerating system consisting of 3.0 mM glucose-6-phosphate, 3.0 U mL^{-1} glucose-6-phosphate dehydrogenase, and 100 μM NADPH). Farnesol, lauric or palmitic acid (250 μM) was added to this and it was incubated with 1–10 μL aliquots (0.65–13.3 μM) of each enzyme separately for 1–30 min to measure the individual enzyme activities. Length of incubation time was chosen based on the activity of each enzyme, so as to yield sufficient products for full characterization. The reactions were stopped by adding 200 μL of 3 N HCl. For lauric and palmitic acid assays, the reaction products were extracted with 6 mL of diethyl ether and were methylated with diazomethane (Sigma-Aldrich, St. Louis, MO, USA) in order to convert the carboxylic acid to its methyl ester. For farnesol the reaction products were extracted using a 200 μg C18 solid-phase extraction column (Honeywell Burdick and Jackson, Morristown, NJ,

Table 2 Mutant protein catalytic activities with cytochrome *c*, NADPH, lauric acid, palmitic acid and farnesol

Protein/substrate	Cytochrome *c* (min^{-1})	NADPH (min^{-1})	Lauric acid (min^{-1})	Palmitic acid (min^{-1})	Farnesol (min^{-1})
CYP102A1	2,980 ± 230	1,650 ± 120	705 ± 35	2,980 ± 140	285 ± 22
				3,160 ± 60[a]	300 ± 8[a]
F87A	3,200 ± 95	1,640 ± 260	303 ± 24	1,840 ± 110	445 ± 15
F87L	3,320 ± 290	1,710 ± 140	233 ± 26	1,270 ± 60	361 ± 26
CYP4C7[b]	–	–	–	–	4.1 ± 0.5[b]
C(73–78)	2,440 ± 380	1,310 ± 90	1.0 ± 0.1	1.2 ± 0.6	35 ± 1
				1.7 ± 0.3[a]	29 ± 2[a]
C(73–78, F87A)	2,330 ± 190	1,100 ± 110	0.6 ± 0.2	0.7 ± 0.2	15 ± 2
C(73–78, F87L)	2,970 ± 110	1,590 ± 120	ND	0.9 ± 0.3	1.5 ± 0.1
C(75–80)	2,880 ± 80	1,650 ± 130	17 ± 2	175 ± 9	7.0 ± 1.2
				190 ± 15[a]	5.3 ± 0.5[a]
C(75–80, F87A)	2,420 ± 130	1,190 ± 140	1.0 ± 0.1	3.1 ± 0.1	4.5 ± 0.5
C(75–80, F87L)	3,170 ± 160	1,750 ± 230	0.9 ± 0.1	6.6 ± 0.9	1.9 ± 0.2
C(78–82)	3,330 ± 270	1,690 ± 110	305 ± 25	2,790 ± 160	345 ± 32
				2,640 ± 340[a]	360 ± 5[a]
C(78–82, F87A)	3,150 ± 140	1,410 ± 80	6.9 ± 0.2	23 ± 1	268 ± 3
C(78–82, F87L)	3,660 ± 270	1,880 ± 140	4.0 ± 0.1	4.0 ± 0.1	1,700 ± 70

Each number is the average of three measurements each for two different expressions of each enzyme, with standard deviations shown

ND not detected

[a] Reference [46]

[b] Reference [47]

USA) and eluted with acetonitrile. The products of the reactions were analyzed by gas chromatography. The integrated areas of the substrate and products peaks were used to calculate the enzyme catalytic reaction rate with substrate. Experimental errors were determined by averaging GC peak areas for 3–5 activity measurements for a given substrate.

Product isolation

A common gas chromatography diagnostic derivatization reagent, *N*,*N*-bis (trimethylsilyl)-2,2,2-trifluoroacetamide (BSTFA) (Sigma-Aldrich), was used to increase the volatility of the reaction products in order to improve their separation [46, 63]. A 500-μL aliquot of BSTFA [5 mg mL^{-1} in dimethylformamide (DMF)] was incubated overnight with the methylated fatty acid reaction mixture before separation by gas chromatography. All of the farnesol metabolites were dried with N_2 gas and dissolved in 200 μL acetonitrile. This concentrated solution of the metabolites was diluted with 100 mM Tris–HCl buffer at pH 7.6 and loaded onto a 200 μg C18 solid-phase extraction column. Epoxyfarnesols were eluted with 2.6 mL of a methanol:water mixture (42:58 ratio) and hydroxyfarnesols were eluted with 3.0 mL of an acetonitrile:water mixture (47:53 ratio). After the removal of solvents, the metabolites were dissolved in tetrahydrofuran for gas chromatography.

Product characterization

The gas chromatography substrate and product peaks were identified using the retention times published previously [1, 2, 46]. The product ratios with lauric acid are shown in the "Electronic supplementary material," Table S3, with palmitic acid in Table S4, and with farnesol in Table S5. The same procedure was used to prepare the products of substrate oxidation for analysis by GC–MS. The temperature of the column oven was programmed as follows: initial temperature was set to 100 °C, held for 2 min, then increased at a rate of 15 °C min^{-1} to 250 °C, and then held for 5 min. Trimethylsilyl (TMS) derivatives of hydroxypalmitic and hydroxylauric acid methyl esters were analyzed by GC–MS. Two groups of ions were used to identify reaction products. The first group was common to all of the hydroxylated fatty acid methyl esters derivatives and are listed as A, B, C and D, respectively, in the "Electronic supplementary material," Table S6 for lauric acid and Table S7 for palmitic acid. The second group includes fragmentation peaks differing by 14 mass units (CH_2), which showed the position of hydroxylation. The products of lauric acid hydroxylation by wild-type CYP102A1 were identified as 12-, 11-, 10-, 9-, 8-, 7- and 6-OH, corresponding to ω to ω-6 hydroxylation, and 15-, 14-, 13-, 12-, 11- and 10-OH for palmitic acid, corresponding to ω-1 to ω-6 hydroxylation, with ω-1 to ω-3 being the major products in both cases.

For farnesol, products were separated first by gas chromatography. All epoxides had very similar retention times and often could not be resolved, while the hydroxylation products had longer retention times than the epoxides, and increased retention times as the hydroxyl group was further displaced from the C1 hydroxyl. Following partial separation of products by gas chromatography, the partially purified products were examined by 1- and 2D NMR spectroscopy in CD_3OD. All of the farnesol metabolites have been identified by NMR spectroscopy and the assignments for each product are shown in the "Electronic supplementary material," Table S8.

Structural model of the C(78–82, F87L) mutant

A homology model of CYP102A1 with the C(78–82, F87L) mutations was built using the software DeepView SWISS-PdbViewer Version 3.7 [64]. The CYP102A1 X-ray structure (PDB code 1FAG) was used as modeling template, in which rotamers were manually selected for each of the mutated residues that did not result in clashes. The structure was manually refined using the Gromos96 [65] implementation in DeepView for local energy minimization (200 cycles of steepest descents followed by 200 cycles of conjugated gradients), first of the mutated residues and then including all the residues within 5 Å. The modeling result was evaluated by the Verify3D [66] and ANOLEA software [67].

Results

Protein characterization

Figure S2a–d of the "Electronic supplementary material" shows the UV/visible spectra of the resting enzymes. In all cases the absorption spectra of the mutant proteins are essentially identical to those of wild-type CYP102A1, suggesting that the mutant proteins fold properly and contain all of the cofactors required for catalysis. All of the proteins have similar reduced CO difference spectra, with a Soret band at 450 nm. An example spectrum is shown in Fig. S3 of the "Electronic supplementary material" for CYP102A1, F87A and F87L. Thus these are typical cytochrome P450 proteins with no detectable P420 inactive form present [61].

MALDI-TOF measurements on CYP102A1 yielded a molecular mass of 117,638 *m/z* within an expected error of ±0.1% (about 118 *m/z*) compared to a calculated molecular mass of the protein of 117,666 Da. This expected error is only slightly smaller than the molecular weight of methionine, 149 minus the mass of H_2O, or 131 Da, and thus it is not certain whether the methionine resulting from the start codon was cleaved during expression in *E. coli*. However, based on the crystal structures of the heme domain [19, 21] (which was expressed, isolated and purified as we have done for the complete holoprotein), the first residue of the heme domain in each case is threonine, thus suggesting that the M0 has been cleaved. Therefore, the entire protein mass, including the heme and the flavins, was calculated based on a molecular mass of 119,525 Da.

The iron and sulfur content of CYP102A1 and its F87A and F87L mutants were measured by ICP spectrometry [60]. The molar S/Fe ratio in the three proteins was extremely similar (36.91 ± 0.96, 37.25 ± 1.26, 37.26 ± 1.26, respectively), which indicates that the mutants have the same Fe loading as the wild-type protein (detailed results are presented in the "Electronic supplementary material," Table S2). This gives an overall average S/Fe ratio of 37.14 ± 0.39. CYP102A1 contains 36 sulfur atoms (9 cysteines and 27 methionines, not including the M0 that results from the start codon of the recombinant gene, which we believe is not present in our enzymes), thus, based on the ICP results, the CYP102A1 proteins studied contain about 3.1% apoprotein. These results also permit the calculation of the extinction coefficients of the heme in the resting protein; at 418 nm ε_{418} was calculated to be 121.0 ± 3.4 mM^{-1} cm^{-1}. The ε_{418} value for the resting enzyme includes the contribution from the flavins present, and provides a simple, rapid method for determining the concentration of CYP102A1.

Catalytic activities of the mutant proteins toward the reduction of cytochrome *c* and oxidation of NADPH and the substrates laurate, palmitate and farnesol were measured as described in the "Materials and methods" section, and are presented in Table 2. The cytochrome *c* reductase activity of wild-type CYP102A1 measured in this work (2,980 ± 230 min^{-1}) is very similar to that reported by Klein and Fulco [6] (2,945 ± 96 min^{-1}) and by Murataliev and Feyereisen [58] (3,200 min^{-1}) under the same conditions. Thus, NADPH transfers electrons well through these enzymes to cytochrome *c*, with a stoichiometry of one NADPH per two cyt *c*. Among the chimeric enzymes of this study, the cytochrome *c* reductase and NADPH oxidase activities are each fairly similar, with three exceptions [C(73–78), C(73–78, F87A) and C(75–80, F87A)], which had lower activities at about 75% of wild-type CYP102A1 and slightly low activity toward all three substrates tested. However, their optical spectra in the resting state ("Electronic supplementary material," Fig. S2, C1 and D2 for the point mutants) do not suggest any detectable lack of flavin absorbance between 450 and 500 nm.

With respect to the monooxygenase activity toward the substrates, while CYP102A1-F87A and -F87L have twofold to threefold lower activities toward the fatty acids, they have slightly increased activities toward farnesol as

compared to the wild-type enzyme. The catalytic activities toward laurate and palmitate also decreased for the F87 point mutants of the three chimeras of the earlier study [46], and in general more so with F87L [with C(75–80, F87L) being the one exception to this]. The same is true for the substrate farnesol, except for the dramatic increase in catalytic activity of C(78–82, F87L) to a value 5.7-fold higher than wild-type CYP102A1.

Identification of the mixed farnesol metabolites by NMR spectroscopy

According to literature data [46, 68–70], farnesol epoxidation at the 2,3 double bond (Scheme 1) causes changes in the chemical shifts of protons at C1, C2, C4 and C13, as shown in Fig. 1. The NMR resonance at 5.36 ppm (H at C2) disappeared and a new resonance appeared at 2.83 ppm (dd). Two protons at C1 gave resonances at 3.52 and 3.62 ppm. The two methylene protons at C4 appeared as multiplets at 1.44 and 1.65 ppm. The methyl resonance at C13 shifted from 1.67 to 1.27 ppm. Farnesol epoxidation at the 10,11 position affects the chemical shifts of protons at C9, C10, C12 and C15. The resonance at 5.09 ppm (proton at C10) disappeared and a new resonance appeared at 2.68 ppm [69, 70]. The resonance due to the methylene protons at C9 was observed at 1.62 ppm. The methyl resonances at C12 and C15 shifted to 1.21 and 1.18 ppm, respectively.

The NMR sample of the farnesol metabolites produced by the C(78–82, F87L) mutant (after separation, purification and concentration) contained ~90% of a new product which had the GC retention time of 7.31 min. The 1-D and COSY spectra of this sample are shown in the "Electronic supplementary material," Fig. S4. There are two multiplet signals between 2.6 and 2.9 ppm, which are very characteristic of methylene protons in epoxides (see above). The question was whether it was a physical mixture of two (2,3 and 10,11) epoxides with ratio 1:1, or whether two oxidations had taken place in the same molecule. In the first case all three olefin resonances, from protons at C2, C6 and C10, with the ratio of intensities 1:2:1, should be observed in the region 5–5.5 ppm (10- and 6- for the 2,3-epoxy, and 2- and 6- for the 10,11-epoxy). There would be only one peak of the same intensity as this for the protons adjacent to the 2,3- and 10,11-epoxy groups. The pattern of methyl resonances in the case of a physical mixture of two different epoxides is also expected to be different. The observed pattern showed shifts to higher shielding for three methyl groups and one (at C14) did not change its chemical shift. The chemical shifts of protons at C5, C6, C8 and C14 either did not change or were affected very slightly. The facts presented above allow us to assign the new product as (2,3),(10,11)-bis-epoxyfarnesol.

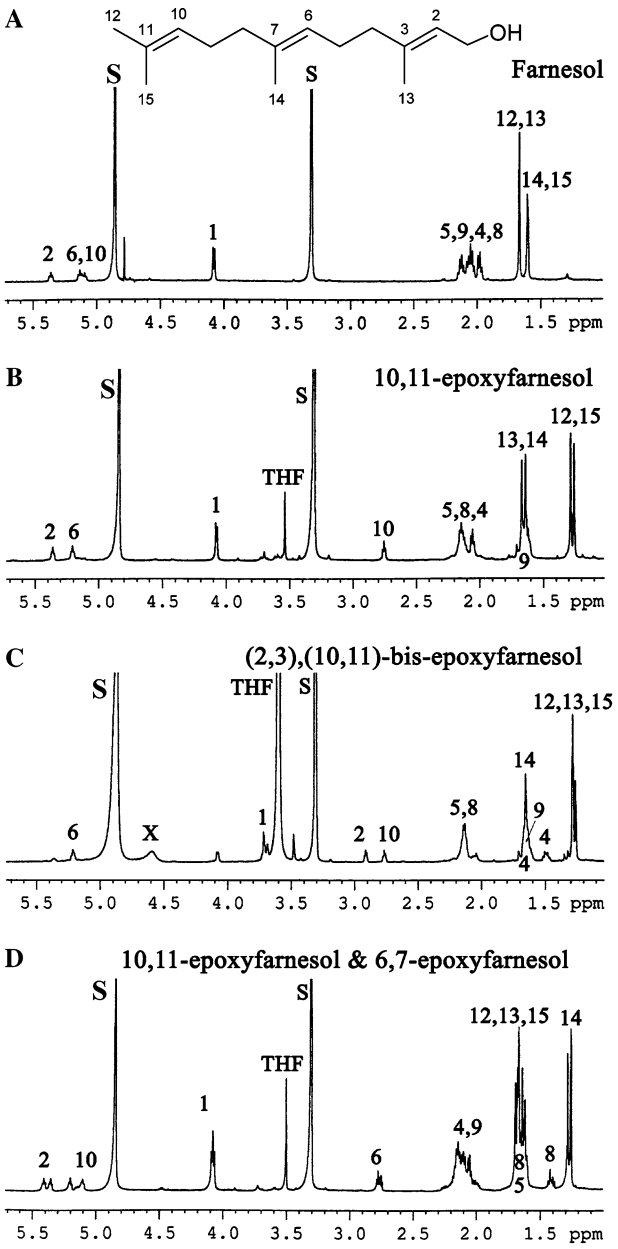

Fig. 1 1D ^{1}H NMR spectra of farnesol and several of its metabolites produced by the mutant enzymes of this study. In **c**, the identity of the broad resonance marked *X* is unknown. In **d**, only the resonances of 6,7-epoxyfarnesol are labeled. Recorded at 600 MHz at 25 °C in CD_3OD

There is a very small amount of another new product in this sample, which has a GC retention time of 7.40 min. This product can be assigned as 10,11-epoxy,9-hydroxyfarnesol, with characteristic resonances at 2.54 ppm (d, 1-CH_2), 3.4 ppm [9-CH(OH)], 2.23 and 2.13 ppm (8-CH_2). Two low-intensity methyl peaks were observed at ~1.3 ppm. The last observation was the key to making the choice between 10,11-epoxy,9-hydroxy- and 6,7-epoxy,5-hydroxyfarnesol, for in the latter case only one peak (M14) would be expected to be shifted from 1.6 to 1.3 ppm.

The NMR sample of the products of farnesol metabolites produced by the C(78–82, F87A) mutant enzyme (after separation, purification and concentration) contained ~90% of two compounds in a 1:1 ratio, which had GC retention times of 6.65 and 6.76 min. The 1-D and COSY spectra of this sample are shown in the "Electronic supplementary material," Fig. S5. The 1-D spectrum contains four triplets (multiplets) in the region 5–5.5 ppm of approximately the same intensity. Two overlapping doublets were observed at 4.1 ppm. Two overlapping resonances appeared in the region where characteristic peaks for epoxides are observed. The methylene resonances completely overlapped. Three of the methyl groups are shifted from 1.66–1.59 to 1.20–1.25 ppm. The other methyl resonances, which were observed at 1.57–1.66 ppm, overlapped with the methylene resonances, and because of this their chemical shifts cannot be measured exactly. The 1-D ^{1}H NMR spectrum of 10,11-epoxyfarnesol, separated from the products of C(78–82, F87L) is shown in Fig. 1b. This spectrum is in good agreement with the assignments reported previously [46]. The comparison of these two spectra allowed one of the metabolites of this sample to be assigned as 10,11-epoxyfarnesol. The other was assigned on the basis of the COSY map of Fig. S4 in the "Electronic supplementary material" and consideration of the spectra of the 2,3- and 10,11-epoxides. The new product was expected to be an epoxyfarnesol because of the very diagnostic resonance at 2.73 ppm, which overlapped in part with the same group at C10 of 10,11-epoxyfarnesol ("Electronic supplementary material," Fig. S5). The same group at the 2C of 2,3-epoxyfarnesol has a larger chemical shift (2.83 ppm), and there is also a very strong coupling between a triplet at 5.36 ppm (2-CH) and a doublet at 4.03 ppm (1-CH_2). Thus 2,3-epoxyfarnesol can be excluded from our consideration. There are some resonances that cannot be considered in connection with the epoxy-specific resonance at 2.73 ppm, because their intensities are too low to be resonances from the same molecule. Three methyl peaks are shifted from ~1.6 to ~1.2 ppm. Two of them belong to 10,11-epoxyfarnesol (M12, M15), the other one can only be from M14 (M13 shift cannot be expected, because 2,3-epoxyfarnesol was already excluded from consideration), and thus the new product was identified as 6,7-epoxyfarnesol.

Metabolite regiospecificity

With *lauric acid* as substrate, wild-type CYP102A1 produces primarily ω-1, ω-2 and ω-3 hydroxylauric acid, while CYP4C7 has no activity with lauric acid ("Electronic supplementary material," Fig. S8) [30, 31]. The chimera C(78–82) shows a similar metabolite ratio to that of the wild-type enzyme and its two F87 mutants all produced 9-hydroxylauric acid as their primary product. C(75–80) and its two F87 mutants all show essentially identical patterns of $9 < 10 < 11$-hydroxylauric acid; hence the F87 residue has no effect on regiospecificity for this chimera. The mutants C(73–78) and C(73–78, F87A) changed the regiospecificity toward the center of the molecule, but the metabolite ratio for C(73–78, F87L) could not be determined because the enzyme is inactive with lauric acid.

With *palmitic acid* as substrate (Fig. 2), wild-type CYP102A1 produces primarily ω-1, ω-2 and ω-3 hydroxypalmitic acid and CYP4C7 shows no activity [46, 47]. The mutant C(78–82, F87L) enhances the production of ω-2 over ω-1 and ω-3 alcohols in a 7.4:4.1:1 ratio, respectively, over that of CYP102A1 (2.1:1.4:1). Overall, all chimeric proteins with the F87 mutation produced ω-2 as the enhanced metabolite, especially for F87L. The chimera C(75–80), which has shown altered regiospecificity toward the center of the substrate, again showed no effect on regiospecificity for its two F87 mutants with palmitic acid. The chimera C(73–78) and its two F87 mutants show altered regiospecificity, but with much lower catalytic activity.

With *farnesol* as substrate (Fig. 3), wild-type CYP102A1 catalyzes farnesol hydroxylation and epoxidation to form 9-hydroxyfarnesol and 2,3- and 10,11-epoxyfarnesol in a 3:2:3 ratio [46], while CYP4C7 produced 12-hydroxyfarnesol as the primary metabolite [47]. The chimera C(78–82) produced the same metabolites as wild-type CYP102A1 [46]. In contrast, for C(78–82, F87L) oxidation of farnesol, only one major metabolite was produced, which was identified by NMR spectroscopy as 10,11-epoxyfarnesol (Fig. 1b). This chimera has very low activity with both lauric and palmitic acids, and thus the substrate selectivity has been altered from medium- and long-chain fatty acids to farnesol. When farnesol was incubated with C(78–82, F87L) for 15 min, this chimeric enzyme had started to form secondary reaction metabolites. The new (secondary) products were identified as 10,11-epoxy,9-hydroxyfarnesol and (2,3),(10,11)-bis-epoxyfarnesol, compared to the primary product 10,11-epoxyfarnesol in a 1:1:4 ratio, respectively. This secondary reactivity appears to be caused by a combination of the alteration of the substrate binding pocket and the higher activity of the C(78–82, F87L) mutant enzyme, which allows the primary metabolite, 10,11-epoxyfarnesol, to re-enter the catalytic site for the secondary oxidation, or to undergo a second oxidation before it can leave the binding pocket. The farnesol metabolites produced by the C(78–82, F87A) mutant enzyme contained ~33% 9-hydroxyfarnesol and ~67% of two epoxides in a 1:1 ratio, which had the GC retention time 6.65 and 6.76 min. One of the products

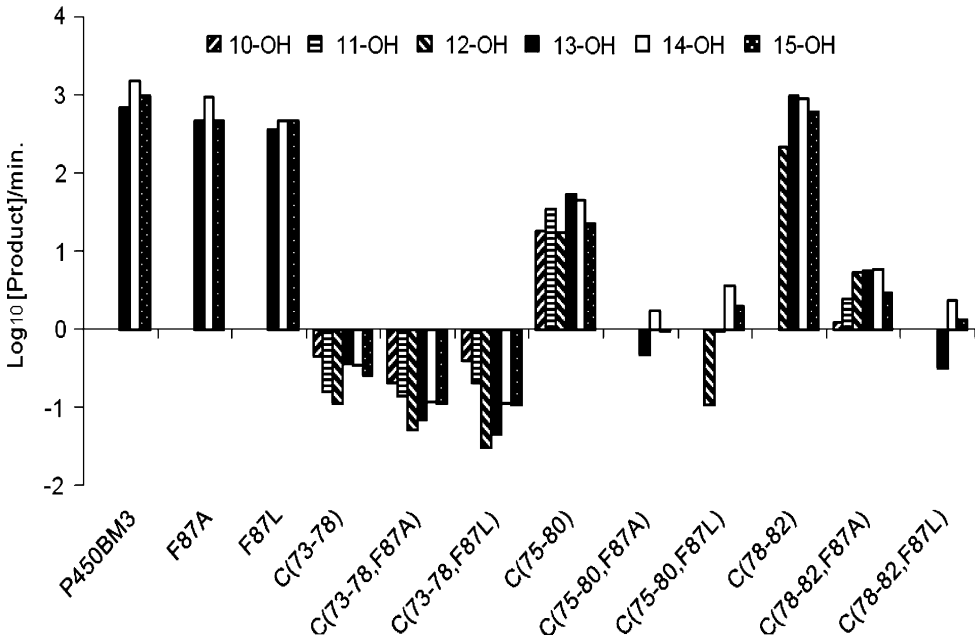

Fig. 2 Logarithm of the turnover number (concentration of products formed per minute from 250 μM palmitic acid oxidation) by 1 μM CYP102A1 or the chimeric proteins. The products formed, as listed in the *key*, are all hydroxypalmitates

was shown to be 10,11-epoxyfarnesol, and the (third) new product was identified as 6,7-epoxyfarnesol.

The chimera C(75–80) has extremely low activity toward farnesol, and the addition of either of the F87 mutations does not increase the activity significantly. The new product 6,7-epoxyfarnesol was also produced by C(73–78, F87L) and C(73–78, F87A). The ability to produce 2,3-epoxyfarnesol and 9-hydroxyfarnesol has been turned off in these chimeric proteins, and they now produce 10,11-epoxyfarnesol as the major metabolite as a result of the addition of F87L or A to the original chimeras [46].

Discussion

In this work we emphasize the role of the additional amino acid F87 that occurs just after the end of the B′-helix of CYP102A1, in a loop that places the phenyl ring above the heme iron (Fig. 4); the three most active chimeras from the "scanning chimeragenesis" study [46] were combined separately with F87A and F87L to create six new chimeric enzymes. We have not attempted to model bound farnesol instead of palmitoleic acid because we do not know whether farnesol binds in an extended or one of many folded conformations. [The patterns of epoxidation at both

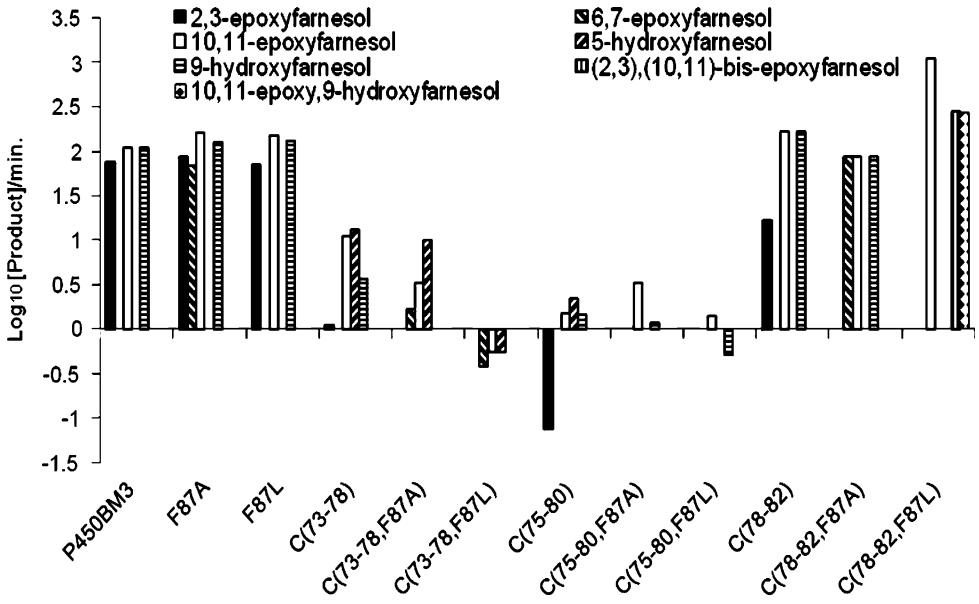

Fig. 3 Logarithm of the turnover number (concentration of hydroxy- and epoxyfarnesol products formed per minute) from 250 μM farnesol during oxidation by 1 μM CYP102A1 or the chimeric enzymes

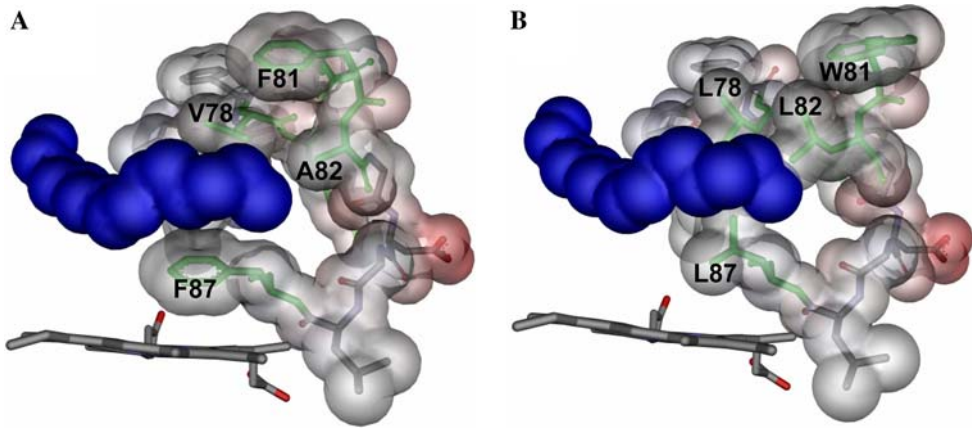

Fig. 4 Residues 73–87 of CYP102A1 (**a**) and the chimeric enzyme C78–82, F87L (**b**) of the substrate binding pocket, with residues 78–82 and 87 colored *green*. The substrate palmitoleate is shown bound to both the wild-type enzyme (**a**) and the chimeric enzyme (**b**). Heme is shown in *stick mode* and palmitoleate in space-filling mode in *blue*; the side chains of the 73–87 peptide are shown in transparent space-filling mode. The figures were created in ViewerLite 5.0 (Accelrys Inc.) and rendered in Pov-Ray (Persistence of Vision Raytracer Pty. Ltd). The homology model (**b**) was generated by DeepView SWISS-PdbViewer [64], as described in the "Materials and methods" section

ends as well as in the center of the molecule have suggested the possibility of folded conformation(s).] As mentioned in the "Introduction," NMR studies [25] have indicated that the conformation of the binding pocket changes upon reduction to the ferrous state, and that the change in conformation allows the substrate to move some 6 Å closer to iron. Thus, our model shown in Fig. 4b is appropriate only in that it provides us with a view of how palmitoleic acid could interact with this part of the substrate-binding pocket of the resting mutant enzyme. In producing this model, the conformation of L82 continually energy-minimized to the extended conformation shown, which is in some conflict with the substrate palmitoleic acid in its observed position in the crystal structure of WT CYP102A1. This causes a slight shift of the substrate in the model of Fig. 4b as compared to 4A, which is consistent with our finding that this mutant enzyme has very low activity with palmitic acid (Fig. 2).

We infer from our experimental results that by changing the shape of the binding pocket from that of Fig. 4a to that of Fig. 4b we have selected against long-chain fatty acids as substrates. We find that the activity of our best chimera, C(78–82, F87L), toward farnesol is 5.7 times greater than that of wild-type CYP102A1. For transition from the resting state to the reduced enzyme for which there is no structure, we are left to conclude that just as the wild-type substrate binding pocket (with substrate relatively far from the iron active site), is able to undergo the changes in conformation necessary to bring the ω-1 to ω-3 carbons of the long-chain fatty acid within reactive reach of the ferryl heme site, the C(78–82, F87L) chimera is able to bring the 10,11-double bond of farnesol to that position so that 10,11-epoxyfarnesol can form as the single primary metabolite. The secondary metabolites of that product tell us that the same or the opposite end of the molecule can be attacked a second time by this highly active enzyme.

All of the F87-mutated chimeric proteins produced fully functional enzymes that catalyzed the hydroxylation of lauric and palmitic acids and farnesol, except for C(73–78, F87L) with lauric acid. Of these, C(78–82, F87L) is most active, while C(75–80, F87L) is *least* active with farnesol. It is remarkable that the same F87 mutation, in combination with two slightly shifted protein fragment replacements, changes the chimeric enzyme activity with the same substrate from lowest to highest. This shows the extreme sensitivity of the substrate binding pocket to seemingly small changes in protein sequence, which allow the accommodation of one substrate, but not another. Residues 75–77 in CYP102A1 are LKF, while in CYP4C7 they are YSF; L75 is within 5 Å of the substrate, while the other two are not. Thus, apparently the Y residue interferes with the binding of farnesol. Residue 78 (within 5 Å of substrate) in CYP102A1 is V, while it is L in CYP4C7, not a large change. In contrast, residues 81 and 82 (both within 5 Å of substrate) of CYP102A1 are FA, but in CYP4C7 they are WL, both of which are much larger, as can be seen by comparing Fig. 4a and b, respectively. Our results show that these two large residues, combined with L87, favor the binding of farnesol significantly.

From published results on the single amino acid mutation of F87 (to A), the hydroxylation of fatty acids was reported to have been shifted from ω-1, ω-2 and ω-3 to the ω position [28], with 12-hydroxylauric acid and 14-hydroxymyristic acid being the major products of those two substrates. The implications of these findings have been quoted and discussed at length [10, 14, 17, 57]. Our results for the single point mutant CYP102A1-F87A agree with the previous report that lauric acid is hydroxylated at the

ω-carbon [28], although in our hands to a *much* smaller extent (3.6%) than the >90% reported. We have not tested myristic acid. However, *neither* palmitic acid *nor* farnesol is hydroxylated at the ω-carbon (Figs. 2, 3), even though farnesol is the same length as lauric acid (Scheme 1). The same is true of the single point mutant CYP102A1-F87L, where *none* of the three substrates of this study shows evidence of ω-hydroxylation.

We have found that although *all* of the F87 mutated chimeric enzymes have altered regiospecificity compared to the wild-type CYP102A1, *most* also have altered regiospecificity compared to the first-generation chimeric proteins [46], as shown in Figs. 2, 3 and Fig. S8 of the "Electronic supplementary material." But *none* of these F87-mutated chimeric enzymes produces ω-hydroxylated products. Thus, this study shows that while chimeragenesis of the 73–87 peptide of CYP102A1 is capable of changing the substrate selectivity from fatty acids to farnesol, on its own it is not sufficient to produce the product of CYP4C7, 12-hydroxyfarnesol. Further investigations of other peptides that make up the substrate binding pocket, and how they may contribute to substrate selectivity and regiospecificity, are in progress.

Acknowledgments We thank Professor Armand Fulco of the University of California Los Angeles for the original *E. coli* strain pbsBM-3 with the plasmid carrying the CYP102A1 gene, Professor Paul Ortiz de Montellano for helpful comments, Dr. Markus Knipp for assistance in the modeling of the chimeras, Dr. Marat B. Murataliev (University of Alberta, Edmonton, AB, Canada) for technical advice on protein purification, fatty acid and farnesol metabolite identification, and Mary T. Flores for preparing the NMR figures. This research was supported by the Walker Research Gift Fund.

References

1. Miura Y, Fulco AJ (1974) Biochim Biophys Acta 249:1880–1888
2. Miura Y, Fulco AJ (1975) Biochim Biophys Acta 388:305–317
3. Narhi LO, Fulco AJ (1986) J Biol Chem 261:7160–7169
4. Fulco AJ (1991) Annu Rev Pharmacol Toxicol 31:177–203
5. Klein ML, Fulco AJ (1993) J Biol Chem 268:7553–7561
6. Klein ML, Fulco AJ (1994) Biochim Biophys Acta 1201:245–250
7. Yeom H, Sligar SG, Li H, Poulos TL, Fulco AJ (1995) Biochemistry 34:14733–14740
8. Murataliev MB, Feyereisen R, Walker FA (2004) Biochim Biophys Acta 1698:1–26
9. Capdevila JH, Wei S, Helvig C, Fulco JR, Belosludtsev Y, Truan G, Graham-Lorence SE, Peterson JA (1996) J Biol Chem 271:22663–22671
10. Munro AW, Leys DG, Mclean KJ, Marshall KR, Ost TW, Daff S, Miles CS, Chapman SK, Lysek DA, Moser CC, Page CC, Dutton PL (2002) Trends Biochem Sci 27:250–257
11. Gilardi G, Meharenna YT, Tsothou GE, Sadeghi SJ, Fairhead M, Giannini S (2002) Biosens Bioelectron 17:133–145
12. Fairhead M, Giannini S, Gillam EM, Gilardi G (2005) J Biol Inorg Chem 10:842–853
13. Dodhia VR, Fantuzzi A, Gilardi G (2006) J Biol Inorg Chem 11:903–916
14. Miles CS, Ost TW, Noble MA, Munro AW, Chapman SK (2000) Biochim Biophys Acta 1543:383–407
15. Li QS, Schwaneberg U, Fisher P, Schmitt J, Pleiss J, Lutz-Wahl S, Schmid RD (2001) Biochim Biophys Acta 1545:114–121
16. Li QS, Ogawa J, Schmid RD, Shimizu S (2001) Appl Environ Microbiol 67:5735–5739
17. Cowart LA, Falck JR, Capdevila JH (2001) Arch Biochem Biophys 387:117–124
18. Li H, Poulos TL (1995) Acta Crystalogr D51:21–32
19. Li H, Poulos TL (1997) Nat Struct Biol 4:140–146
20. Sevrioukova IF, Li H, Zhang H, Peterson JA, Poulos TL (1999) Proc Natl Acad Sci USA 99:1863–1868
21. Haines DC, Tomchick DR, Machius M, Peterson JA (2001) Biochemistry 40:13456–13465
22. Joyce MG, Girvan HM, Munro AW, Leys D (2004) J Biol Chem 279:23287–23293
23. Kuper J, Wong TS, Roccatano D, Wilmanns M, Schwaneberg U (2007) J Am Chem Soc 129:5786–5787
24. Modi S, Primrose WU, Boyle JMB, Gibson CF, Lian L-Y, Roberts GCK (1995) Biochemistry 34:8982–8988
25. Modi S, Sutcliffe MJ, Primrose WY, Lian L-Y, Roberts GCK (1996) Nat Struct Biol 3:414–417
26. Graham-Lorence S, Truan G, Peterson JA, Falck JR, Wei S, Helvig C, Capdevila JH (1997) J Biol Chem 272:1127–1135
27. Shao Z, Arnold FH (1996) Curr Opin Struct Biol 6:513–518
28. Oliver CF, Modi S, Sutcliffe MJ, Primrose WU, Lian LY, Roberts GC (1997) Biochemistry 36:1567–1572
29. Joo H, Lin Z, Arnold FH (1999) Nature 399:670–673
30. Noble MA, Miles CS, Chapman SK, Lysek DA, Mackay AC, Reid GA, Hanzlik RP, Munro AW (1999) Biochem J 339:371–379
31. Li QS, Schwaneberg U, Fisher P, Schmid RD (2000) Chem Eur J 6:1531–1536
32. Loughran PA, Roman LJ, Aitken AE, Miller RT, Masters BSS (2000) Biochemistry 39:15110–15120
33. Arnold FH, Wintrode PL, Miyazaki K, Gershenson A (2001) Trends Biochem Sci 26:100–106
34. Farinas ET, Schwaneberg U, Glieder A, Arnold FH (2001) Adv Synth Catal 343:601–606
35. Glieder A, Farinas ET, Arnold FH (2002) Nat Biotechnol 20:1135–1139
36. Salazar O, Cirino PC, Arnold FH (2003) Chembiochem 4:891–893
37. Kumar S, Chen CS, Waxman DJ, Halpert JR (2005) J Biol Chem 280:19569–19575
38. Meinhold P, Peters MW, Chen MM, Takahashi K, Arnold FH (2005) Chembiochem 6:1765–1768
39. Kumar S, Halpert JR (2005) Biochem Biophys Res Commun 338:456–464
40. Otey CR, Bandara G, Lalonde J, Takahashi K, Arnold FH (2006) Biotechnol Bioeng 93:494–499
41. Kumar S, Sun L, Liu H, Muralidhara BK, Halpert JR (2006) Protein Eng Des Sel 19:547–554
42. Kumar S, Liu H, Halpert JR (2006) Drug Metab Dispos 34:1958–1965
43. Sun L, Chen CS, Waxman DJ, Liu H, Halpert JR, Kumar S (2007) Arch Biochem Biophys 458:167–174
44. Zhao Y, Halpert JR (2007) Biochim Biophys Acta 1770:402–412
45. Peters MW, Meinhold P, Glieder A, Arnold FH (2003) J Am Chem Soc 125:13442–13450
46. Murataliev MB, Trinh LN, Moser LV, Bates RB, Feyereisen R, Walker FA (2004) Biochemistry 43:1771–1780
47. Sutherland TD, Unnithan GC, Andersen JF, Evans PH, Murataliev MB, Szabo LZ, Mash EA, Feyereisen R (1998) Proc Natl Acad Sci USA 95:12884–12889

48. Baker FC, Mauchamp B, Tsai LW, Schoolery DA (1983) J Lipid Res 24:1586–1594
49. Bede J, Goodman WG, Tobe S (1999) Pure Appl Chem 70:1–9
50. Yu SJ (2000) Zool Stud 39:243–249
51. Helvig C, Koener JF, Unnithan GC, Feyereisen R (2004) Proc Natl Acad Sci USA 101:4024–4029
52. Raner GM, Muir AQ, Lowry CW, Davis BA (2002) Biochem Biophys Res Commun 293:1–6
53. Barchuk AR, Maleszka R, Simoes LP (2004) Insect Mol Biol 13:459–467
54. Boddupalli SS, Pramanik BC, Slaughter CA, Estabrook RW, Peterson JA (1992) Arch Biochem Biophys 292:20–28
55. Pearson WR (1996) Meth Enzymol 266:227–258
56. Gotoh O (1992) J Biol Chem 267:83–90
57. Li H, Poulos TL (1999) Biochim Biophys Acta 1441:141–149
58. Murataliev MB, Feyereisen R (1996) Biochemistry 35:15029–15037
59. Morrison HG, Desrosiers RC (1993) Biotechniques 14:454–457
60. Bongers J, Walton CD, Richardson DE, Bell JU (1988) Anal Chem 60:2683–2686
61. Omura T, Sato R (1964) J Biol Chem 239:2379–2385
62. O'Keeffe DH, Ebel RE, Peterson JA (1978) Methods Enzymol 52:151–157
63. Nicolaides N, Soukup VG, Ruth EC (1983) Biomed Mass Spectrom 10:441–449
64. Guex N, Peitsch MC (1997) Electrophoresis 18:2714–2723
65. van Gunsteren WF et al (1996) Biomolecular simulation: the GROMOS96 manual and user guide. vdf Hochschulverlag AG an der ETH Zürich, Zürich/BIOMOS BV, Groningen
66. Luthy R, Bowie JU, David Eisenberg D (1992) Nature 356:83–85
67. Melo F, Feytmans E (1998) J Mol Biol 277:1141–1152
68. Davis CE, Bailey JL, Lockner JW, Coates RM (2003) J Org Chem 68:75–82
69. Hanzlik RP (1988) Org Synth Coll 6:560–565
70. Hanzlik RP (1977) Org Synth Coll 56:112–115